J Solid State Electrochem (2008) 12:715–720
DOI 10.1007/s10008-007-0414-1

ORIGINAL PAPER

Different methods of preparing electrode from single-wall carbon nanotubes and their effect on the Li ion insertion process

I. Mukhopadhyay · H. Touhara

Received: 25 May 2007 / Revised: 13 August 2007 / Accepted: 18 August 2007 / Published online: 12 September 2007

Abstract Single-wall carbon nanotube (SWNT) is processed in three different ways: (1) coating a film out of a slurry of SWNT with poly (vinilydene difluoride) (PVDF) binder on to a Cu substrate, (2) evaporating SWNT dispersion in methanol on to a Cu substrate, and (3) transferring a film on to a Cu substrate from the water–ethanol interface, to prepare the working electrode for studying the Li ion insertion process. The use of binder enhances irreversible capacity restricting the Coulomb efficiency to only 18% in the initial cycle. The electrode prepared by deposition of SWNT powder from a dispersion of methanol on the Cu substrate gives the best reversible capacity of 445 mA h g^{-1} and Coulomb efficiency of 25% in the initial cycle. Use of the PVDF binder favors the formation of thicker solid electrolyte interface, which counts the large irreversible capacity.

Keywords Li ion battery · Carbon nanotube · Li ion insertion · Reversible capacity

Introduction

Li ion batteries became a very important power source for portable electronic devices in our modern daily life. Although Li metal holds great promise of delivering a theoretical capacity of 3,860 mA h g^{-1} as a negative electrode material, it is known that graphitic carbon is actually used [1–3]. Use of graphitic carbon limits the available reversible capacity to only 372 mA h g^{-1} (corresponding to a saturation composition of LiC_6); however, many practical problems, e.g., solvent exfoliation and dendrite formation are avoided [4]. Hence, there has been a constant search for active negative electrode material that can provide better reversible capacity than graphitic carbon while retaining the same order of stability (cycle efficiency). In this regard, carbon nanotubes, with an interesting one-dimensional host lattice structure, have been studied by several groups [5–15]. Two types of carbon nanotubes have been studied for the purpose. Multiwall carbon nanotubes, resembling Russian doll structure, have been found to show fairly high reversible capacity with very high irreversible capacity in the initial cycle [5–9]. However, the reversible capacity diminishes fast with successive cycles [7]. On the contrary, single-wall carbon nanotube (SWNT) forms a rope structure consisting of a large number of individual tubes [10, 11, 13]. These rope structures exhibit a 2D triangular lattice offering huge interstitial sites for Li ion insertion/absorption. SWNT ropes have been reported to show a maximum reversible capacity in the range of 450–600 mA h g^{-1} [10]. Further treatment of the SWNT ropes by mechanical ball milling enhances the reversible capacity to 1,000 mA h g^{-1} [12]. Chemical etching of SWNTs to variable lengths enhanced the reversible Li storage capacity from a saturation composition of LiC_6 (corresponding to a reversible capacity of 372 mA h g^{-1}) in close-end SWNTs to LiC_3 (reversible capacity of 744 mA h g^{-1}) after etching, which is twice the value observed in intercalated graphite [16]. However, the irreversible capacity is reported to be very high in case of SWNT also [10, 12, 15]. Moreover, it is shown that mechanical ball milling of SWNT ropes reduces the irreversible capacity from 1,190 to 484 mA h g^{-1} [12].

I. Mukhopadhyay (✉)
Materials Chemistry, Salt and Marine Chemicals Division,
CSMCRI,
Gijubhai Badheka Marg,
Bhavnagar 364 002 Gujarat, India
e-mail: indrajit@csmcri.org

H. Touhara
Faculty of Textile Science and Technology, Shinshu University,
Ueda 386 8567 Nagano, Japan
e-mail: htohara@giptc.shinshu-u.ac.jp

Therefore, in general, we found that carbon nanotubes offer a huge possibility with few serious drawbacks namely, huge irreversible capacity in the initial Li insertion process and fading of reversible capacity with time. Many studies have been carried out to overcome these drawbacks, but most of them are concerned with either the control of the structure of SWNTs by various preparative ways [10, 13, 15] or further treatment of the SWNT ropes to induce defects, etc. [12, 16].

In the present communication, we report on three different ways of preparing working electrodes (WEs) namely, using binder, depositing SWNT from a dispersion of methanol on to Cu electrode, and transferring a film of SWNT on to Cu substrate from the interface of water and methanol, from SWNT powder. The effect of the presence of binding material on the reversible Li ion insertion process is discussed. The Li ion insertion process in thin film of the SWNT electrode, obtained by the organization of carbon nanotubes, without any binder is also looked at.

Materials and methods

SWNTs were prepared by passing a dc arc between a composite graphite anode and a pure graphite cathode in He atmosphere [15]. Crude SWNT was purified by refluxing in 0.1 M HNO_3 and subsequent washing in mili-Q water. The washed residue was dried at 100 °C and finally calcined in vacuum at 300 °C. The SWNTs content of the final residue, which was used for the present study, was 80% [15]. The Brunauer–Emmett–Teller surface area of the SWNTs under present investigation was 100 $cm^2\ g^{-1}$. X-Ray powder diffraction of the SWNT powder did not show any characteristics diffraction line corresponding to the 2D triangular lattice of the ropes. Scanning electron microscopy showed mat type appearance of the surface of the SWNTs powder. The structure of the SWNT bundle was analyzed by a JEOM JEM-2010 transmission electron microscope (TEM) operated at 200 kV with a point-to-point resolution of 0.19 nm. Scanning electron microscopic studies were carried out with a Hitachi S-5000 machine. The Raman studies were performed by a Renishaw Raman spectrometer 3000 using monochromatic radiation of 632.8 nm from a He–Ne ion laser at an incident power of 25 mW.

All the electrochemical measurements were done using a three-electrode cell configuration with SWNT, processed in three different ways, as the WE, a Li foil connected to Cu wire as the coated electrode, and the reference electrode. $LiClO_4$ (1 M) dissolved in 1:1 (v/v) ethylene carbonate and diethyl carbonate was used as the active electrolyte for all electrochemical measurements. The cells were assembled in a dry box filled with Ar. In the present test cells, Li was inserted into the SWNT WE during the discharge. The WE was made by three different ways using SWNTs powder: (1) WE1, prepared by coating a slurry made of 4.5 mg of SWNTs and 0.5 mg of 10 wt% PVDF binder in the ratio of 90:10, (w/w) diluted by *N*-methyl-2-pyrolidinone, on one side of a Cu current collector; the surface area of the coated electrode was 1 cm^2, and the approximate thickness was 10 μm; (2) WE2, made by the deposition of SWNTs from its colloidal suspension, made by dispersing 2 mg of SWNT powder in 10 ml of methanol, on a Cu foil electrode; the thickness of the active carbon material was 0.8 μm; and (3) WE3, prepared by transferring film of SWNTs for several times, formed on the interface of air and 1:1 (v/v) H_2O–methanol mixture, on one side of a Cu current collector; the thickness of the active SWNT layer was 0.6 μm. Before the electrochemical studies the electrodes were dried at 120 °C under vacuum overnight. Galvanostatic discharge–charge measurements were done in a Swagelok-type cell using a polypropylene celgard between the WE and the Li counter electrode. The geometric surface area of the WE was maintained at 1 cm^2. The average weight of active carbon material in the WEs was kept on an average 0.08–0.05 mg. The potential range for the charge–discharge measurements were kept in 0–2.5 V at an applied current density of 50 mA g^{-1}. Cyclic voltammetry (CV) studies were performed in a glass cell at a sweep rate of 0.1 mV s^{-1}. All the electrochemical measurements were performed in a dry box using Ar atmosphere where the average oxygen and moisture content was less than 20 ppm.

Results and discussion

Characterization of single wall nanotubes

TEM image of the SWNTs is shown in Fig. 1. Bundles of SWNTs are observed with the presence of amorphous carbon and carbon-coated catalyst particles. The average diameter of the individual nanotubes is approx. 1.46 nm. The bundles are approx. 8–30 nm in diameter containing approx. 30–450 individual nanotubes. The graphite planes are wrinkled and show the presence of surface defects. We do not find a rope structure in the SWNT bundles through the TEM. The X-ray diffraction result also supports the finding of the TEM studies [15]. Collection of SWNT bundles is shown through the scanning electron micrograph shown in Fig. 2. The catalyst particles were found to be coated with amorphous carbon. The diameter of the individual nanotube is calculated from the radial breathing mode (rbm) of the Raman spectra, which is shown in Fig. 3. The diameter of the individual nanotubes is calculated as 1.50 nm using a wave number of 163 cm^{-1} as the rbm [17]. The SWNTs are found moderate graphitized as indicated by the higher intensity of the band at 1,589.7 cm^{-1}, which is attributed to one of the E_{2g} (the G

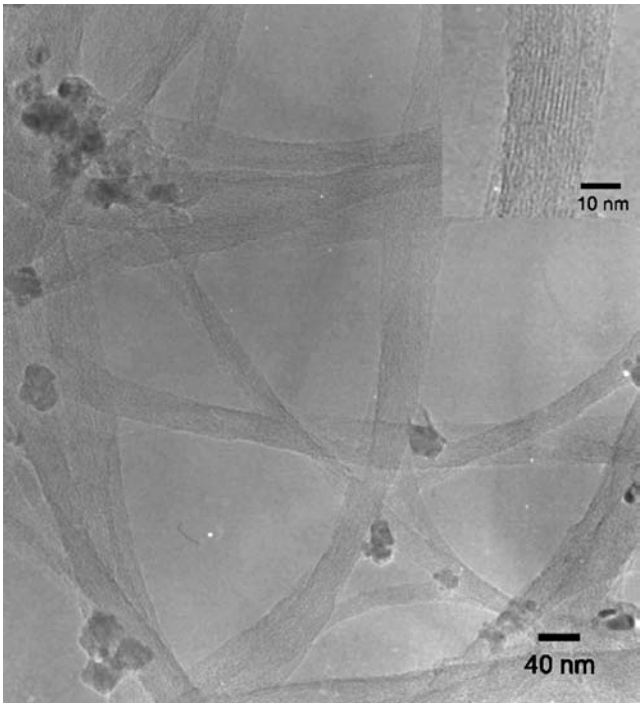

Fig. 1 TEM image of SWNT bundle. The *inset* shows the high-resolution picture of individual SWNTs

band) modes of highly oriented pyrolytic graphite [18]. The other band at 1,324.9 cm^{-1} is attributed to the disorder-induced D-band of graphite.

Galvanostatic charge–discharge measurements

Potential profiles from the galvanostatic charge–discharge studies are presented in Fig. 4. The common feature of all the three potential profiles is the occurrence of huge irreversible capacity, in the initial Li insertion process and hysteresis between consecutive charge–discharge cycles.

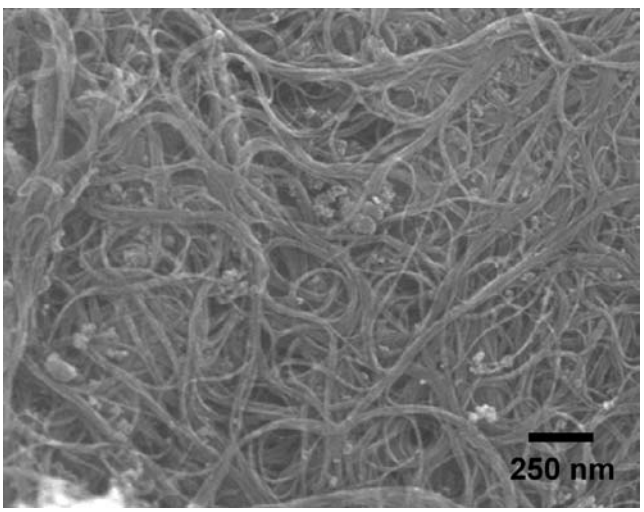

Fig. 2 SEM image of SWNT bundles. The bundle structure of SWNT is found to have amorphous carbon-coated catalyst particles

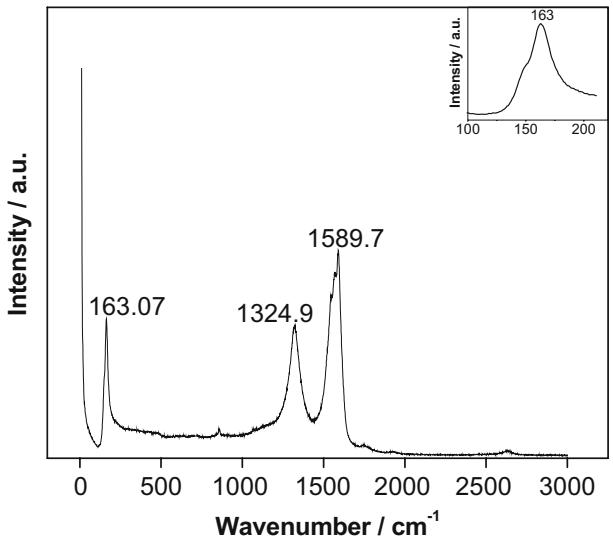

Fig. 3 Raman spectra of SWNT powder at an excitation wavelength of 632.8 nm. The *inset* shows the rbm

Because the SWNT in the present study was treated at a maximum temperature of 300 °C and were found to contain amorphous carbon along with catalyst particles, the hysteresis of the potential profiles can be attributed to the activated processes such as the formation of Li–C–H or C–O–Li species [8, 13]. Huge irreversible capacity in the initial Li insertion process is seemed to be contributed by various processes to a different degree for the three different electrodes. In the case of WE1, we note two different pseudopotential plateaus at 1.4 and 1.0 V, which are mainly contributing to the irreversible capacity in the initial Li insertion step. It is noted that the plateau at 1.4 V is actually started at 1.9 V. The electrochemical process associated with the pseudoplateau above 1.5 V is generally attributed to the reduction in surface-oxygenated species to form oxides of Li [8]. The pseudopotential plateau at 1.4 V

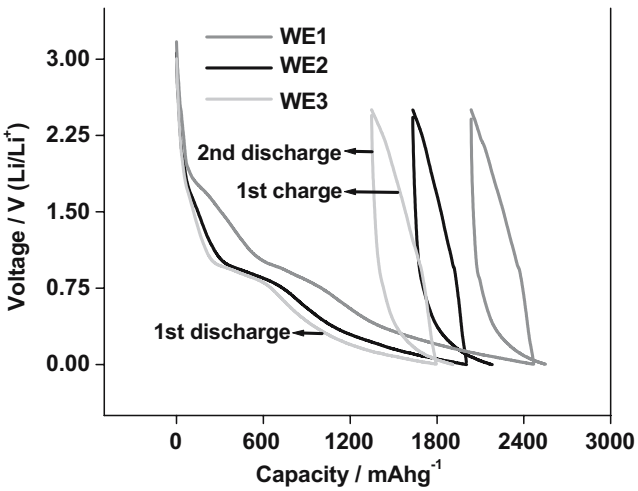

Fig. 4 Galvanostatic charge–discharge profiles of SWNTs electrodes at a current of 50 mA g^{-1}. The SWNT content of WE1, WE2, and WE3 was 0.08, 0.05, and 0.04 mg, respectively

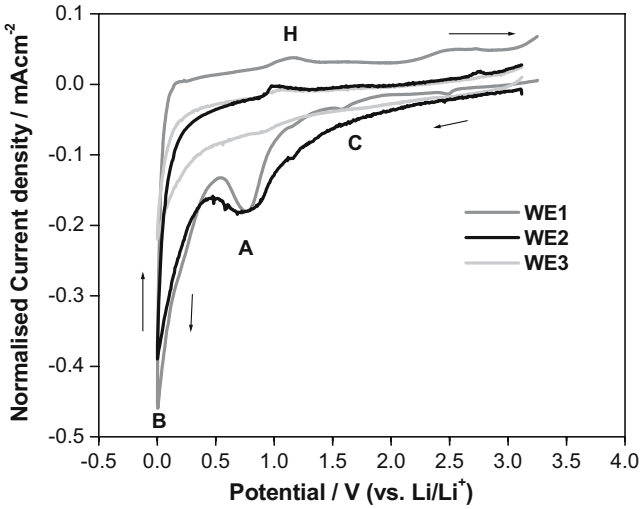

Fig. 5 CV for the initial Li insertion/extraction process (the first cycle) for WE1 and WE2 at a sweep rate of 0.1 mV s^{-1}. The electrode area is 1 cm^2, and SWNT content of WE1, WE2, and WE3 are 0.08, 0.05, and 0.04 mg

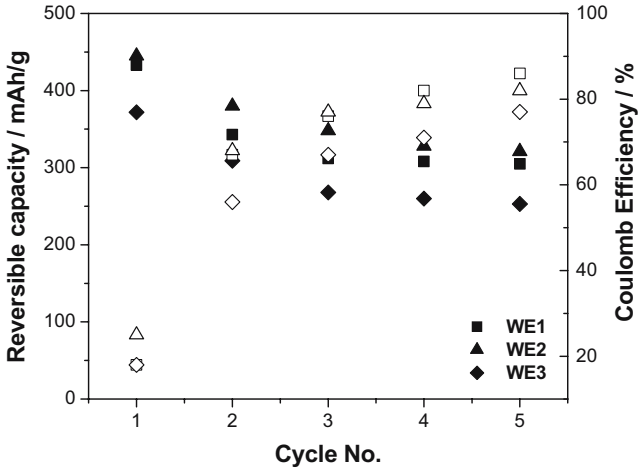

Fig. 7 Variation of reversible charge capacities (*solid symbols*) and Coulomb efficiencies (*empty symbols*) with the number of cycle, obtained from continuous charge–discharge measurement

is correlated with the reduction in solvent, while the other at 1.0 V is attributed to the formation of protective layer, SEI along with the reduction in solvent [7, 8]. Similar processes are also found to occur in the case of WE2 and WE3. Two distinct pseudopotential plateaus are observed at 1.2 and 1.0 V for both the electrodes. A closer look in Fig. 3 clearly indicates that the potential profile for WE1 electrode differs a large extent from those of WE2 and WE3. In the case of WE1, the contribution of irreversible processes associated with the reduction in surface-oxygenated species and formation of SEI is larger than those of WE2 or WE3. Thus, the use of binder for the electrode preparation modifies the surface of the SWNT powder by introducing surface-oxygenated species. Moreover, larger contribution to the irreversible capacity through the potential plateau at 1.0 V for WE1 and WE3 may be explained on the basis of larger accessible active surface of SWNT for the formation of the SEI film [8]. We found that the irreversible capacity for the initial Li insertion process is 2,034 mA h g^{-1} for WE1 compare to 1,348 and 1,632 mA h g^{-1} for WE2 and WE3, respectively. A comparison between the potential profiles of WE2 and WE3 reveals that the reversible Li insertion is more facile in the WE2 than WE3. The larger irreversible capacity of WE3 than WE2 may be correlated to the excess surface oxygen species, as seen from the potential inflection at 1.4 V, present on the WE3 electrode [8].

Cyclic voltammetry

The process of Li ion insertion and extraction into/from the SWNTs was further studied by CV for all the three electrodes. Shown in Fig. 5 is a comparison of the CVs for the initial Li ion insertion/extraction process (first cycle) for the three electrodes. All the electrodes show few similar features in the CV of the initial Li insertion process. The current peak "A" in Fig. 5 is attributed to the formation of the SEI film on the surface of the electrode along with partial contribution from the reduction in solvent [13]. The Li ion insertion process is found to take place in the whole range of potential from 3 to 0 V [13]. In the positive sweep, we note that the extraction of Li ion occurs in the whole

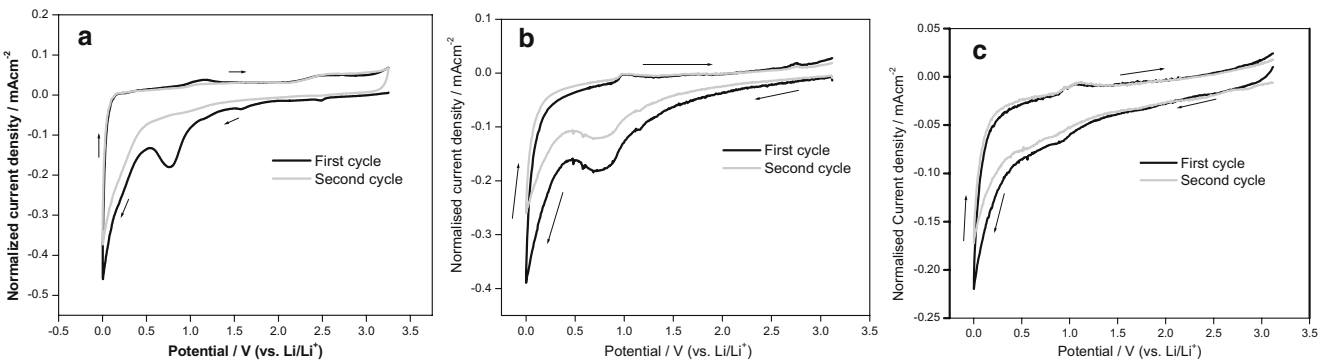

Fig. 6 CVs showing the initial two consecutive cycles for Li insertion/extraction process for **a** WE1 **b** WE2, and **c** WE3 at a sweep rate of 0.1 mV s^{-1}

range of potential from 0 to 3 V in case of WE1, which rules out the possibility of any staging transition in the SWNTs, which is normally encountered in graphitic carbon [13]. Further, absence of any defined redox peak for the Li intercalation process clearly indicates that the mechanism of Li ion insertion is entirely different in the case of SWNT electrodes [13, 19]. In the case of WE2, the Li extraction process is completed in a relatively narrow potential range of 0–1.2 V. The normalized current density of WE2, in Fig. 5, is lower than WE1 indicating weak contact (ohmic) among the SWNT and between SWNT to the Cu substrate. Apart from solvent reduction and SEI formation, we do find the occurrence of some other processes also at current peak A. The additional process is partially reversible in nature as it gives a current hump C in the anodic sweep. A comparison of the CV of WE1 and WE2 clearly shows a larger contribution of capacity toward the irreversible processes by WE1 than WE2. The CV of WE1 in the potential range of open-circuit potential to 1.5 V (till region "B" in Fig. 5) shows that the unwanted irreversible processes, associated with the presence of oxygenated functionalities on the surface, are enhanced. However, the fact that is of further interest is the larger contribution of current to charge the electrochemical double layer (ECDL) by WE1. This observation can be correlated to the porous nature of the SEI formed over the WE1 electrode [8]. The porous nature of WE1 can further be supported from the CV for the first two consecutive cycles for the same electrode, which is shown in Fig. 6a. It is noted that the current contribution to charge the ECDL is substantial in the second cycle also. The first two consecutive cycles for WE2 and WE3 show almost similar behavior. Another interesting observation, common to all the three electrodes, is that the charge consumed for the SEI formation or total irreversible capacity associated with the SEI formation is the highest in the first cycle and decreases in the subsequent cycles. Both WE2 and WE3 show an appreciable current in the second cycle, associated with the growth of SEI—a feature that is not observed with WE1.

Continuous charge–discharge measurements

The performance of the three electrodes for the first five consecutive cycles was continuously recorded through galvanostatic discharge–charge measurement, and the results are shown in Fig. 7. It is noted that the reversible capacity for WE1 and WE2 are comparable namely, 433 and 445 mA h g^{-1}, respectively, while WE3 shows a reversible capacity of only 372 mA h g^{-1}. The Coulomb efficiency of WE2 in the initial cycle is recorded to be the highest ,i.e., 25%, among the three different electrodes. It is observed that the reversible charge capacity decreased by 30% of its initial value for WE1 after five cycles, while it is 28% for WE2. Thus, the electrode prepared by deposition of SWNT on to the Cu substrate from dispersion in methanol performed in a better way in terms of reversible capacity, Coulomb efficiency, and cycle stability. The electrode prepared by transferring the film of SWNT on to the Cu substrate from the interface shows the lowest charge capacity, Coulomb efficiency, and cycle stability.

Conclusions

SWNT is processed in three different ways to fabricate electrodes for studying the Li intercalation/insertion process. It is found that the electrode prepared by using the PVDF binder, WE1, modifies the surface by introducing surface-oxygenated species and shows a maximum irreversible capacity of 1,601 mA h g^{-1}. The use of the PVDF binder, although giving better connectivity, is found to introduce surface-oxygenated species and facilitates thicker but porous SEI, which in turn enhances the irreversible capacity. Electrode WE3, prepared by transferring the film from the air–solvent interface to the Cu substrate, is found to give reversible capacity of 372 mA h g^{-1} and Coulomb efficiency of 18%. It may be speculated that weak ohmic contact among the SWNT particles and to the Cu substrate leads to such observation. Electrode WE2, prepared by deposition of SWNT on to the Cu substrate from a dispersion of methanol, has shown the best reversible charge capacity of 445 mA h g^{-1} with highest Coulomb efficiency of 25%, although the CV result indicates weak ohmic contact among the particles. Therefore, the results clearly indicate that the processing of the SWNT powder to the actual electrode configuration plays a major role in determining the performance of the Li ion battery.

Acknowledgments The financial support in the form of a fellowship from the JSPS, Japan, to carry out the work is gratefully acknowledged. Thanks are due to the Shinshu University, Udea-shi, Japan, for providing the facility to complete the experimental work. Thanks are due to the Director, CSMCRI, Bhavnagar, for his keen interest in the present work.

References

1. Broussely M, Archdale G (2004) J Power Sources 386:136
2. Levi MD, Aurbach D (1997) J Electroanal Chem 421:79
3. Tanaka U, Sogabe T, Sakagoshi H, Ito M, Tojo T (2001) Carbon 39:931
4. Fong R, von Sacken U, Dahn JR (1990) J Electrochem Soc 137:2009
5. Frackowiak E, Gautier S, Gaucher H, Bonnamy S, Beguin F (1999) Carbon 37:61
6. Maurin G, Bousquet Ch, Henn F, Bernier P, Almariac R, Simon B (2000) Solid State Ion 136–137:1295

7. Wu GT, Wang CS, Zhang XB, Yang HS, Qi ZF, He PM, Li WZ (1999) J Electrochem Soc 146:1696
8. Beguin F, Metenier K, Pellenq R, Bonnamy S, Frackowiak E (2000) Mol Cryst Liq Cryst 340:547
9. Mukhopadhyay I, Hoshino N, Kawasaki S, Okino F, Hsu WK, Touhara H (2002) J Electrochem Soc 149:A39
10. Gao B, Kleinhammes A, Tang XP, Bower C, Fleming L, Wu Y, Zhou O (1999) Chem Phys Lett 307:153
11. Zhao J, Buldum A, Han J, Lu J (2000) Phys Rev Lett 85:1706
12. Gao B, Bower C, Lorentzen JD, Fleming L, Kleinhammes A, Tang XP, McNeil LE, Wu Y, Zhou O (2000) Chem Phys Lett 327:327
13. Claye A, Fischer JE, Huffman CH, Rinzler AG, Smalley RE (2000) J Electrochem Soc 147:2854
14. Aurbach D, Gnanaraj JS, Levi MD, Levi EA, Fischer JE, Claye A (2001) J Power Sources 97–98:92
15. Mukhopadhyay I, Kawasaki S, Okino F, Govindaraj A, Rao CNR, Touhara H (2002) Physica B 323:130
16. Shimoda H, Gao B, Tang XP, Kleinhammes A, Fleming L, Wu Y, Zhou O (2001) Phys Rev Lett 88:015502
17. Dresselhaus MS, Dresselhaus G, Eklund PS (1996) Science of fullerenes and carbon nanotubes. Academic, San Diego
18. Tuinstra F, Koenig JL (1970) J Chem Soc 53:1126